MDPI

Article

Desorption and Reuse of Pb-BHA-NaOL Collector in Scheelite Flotation

Jianjun Wang [1,2,3], **Zhiyong Gao** [1,2,3,*] and **Wei Sun** [1,2,3,*]

1. School of Minerals Processing and Bioengineering, Central South University, Changsha 410083, China; jianjunwang@csu.edu.cn
2. Key Laboratory of Hunan Province for Clean and Efficient Utilization of Strategic Calcium-Containing Mineral Resources, Central South University, Changsha 410083, China
3. Hunan International Joint Research Centre for Efficient and Clean Utilization of Critical Metal Mineral Resources, Central South University, Changsha 410083, China
* Correspondence: zhiyong.gao@csu.edu.cn (Z.G.); sunmenghu@csu.edu.cn (W.S.)

Abstract: Pb and BHA in Pb-BHA-NaOL collector assembled by lead nitrate (Pb), benzohydroxamic acid (BHA), and sodium oleate (NaOL) with a 240:120:1 molar ratio in scheelite flotation have the common defects of flotation reagents including high cost, environmental pollution and reducing hydrometallurgy efficiency. Therefore, in this study, the efficient desorption and reuse of Pb and BHA adsorbed on the scheelite surfaces was first proposed. The desorption test results showed that 80.71% Pb and 70.93% BHA could be efficiently desorbed from the scheelite concentrate surfaces through strong stirring for 15 min at pH 13.0 and a speed of 1600 r/min. The reuse of the desorbed collector could save 67% Pb and 75% BHA. The results of desorption and reuse tests of the real ore also exhibited high feasibility in industrial application. Fourier transform infrared spectroscopy analysis revealed that Pb-O, C=O, and C-N groups of Pb and BHA adsorbed on the scheelite surfaces obviously weakened or disappeared. Atomic force microscopy analysis further confirmed that most of the Pb and BHA on the scheelite surfaces were removed. Therefore, this work not only solves the above defects of the collector but also provides a reference for the desorption and reuse of other flotation reagents.

Keywords: scheelite; flotation; Pb-BHA-NaOL collector; desorption; reuse

1. Introduction

As a strategic calcium mineral, scheelite ($CaWO_4$) is widely used in alloys, steel, chemical compounds, and tools [1]. Generally, the content of scheelite in the ore body is very low, so it must be separated from fluorite and other gangue minerals and enriched to be a scheelite concentrate with a high grade before tungsten hydrometallurgy [2]. The traditional separation methods of scheelite from gangue minerals include gravity separation and froth flotation [3]. Froth flotation is the most commonly used method due to its high separation efficiency and adaptability for fine ores [4]. Sodium oleate (NaOL) is a typical fatty acid collector widely used in oxide minerals [5]. Benzohydroxamic acid (BHA) is a hydroxamic acid collector and has a good selectivity for scheelite when making it assemble with lead nitrate (Pb) [6]. Therefore, NaOL and the mixture (Pb-BHA) of Pb and BHA are the main collectors in scheelite flotation [7–10]. The NaOL collector has the characteristics of strong collecting ability and poor selectivity, while the Pb-BHA collector possesses the opposite characteristics [11–13]. Therefore, the Pb-BHA-NaOL collector assembled by Pb, BHA, and NaOL with a special sequence and 240:120:1 molar ratio was developed in our previous study [14]. However, the costs and contents of Pb and BHA in the Pb-BHA-NaOL collector are far higher than those of NaOL [15]. Moreover, Pb^{2+} is a heavy metal ion and BHA contains the benzene ring, harmful to the human body, and the hydrometallurgy

process of scheelite [16–18]. Thus, it is of significance if Pb and BHA on the scheelite concentrate surfaces can be desorbed and reused efficiently.

The common desorption methods of collectors on minerals include the physical method, chemical method, and physicochemical combination method [19]. The physical method is usually used to treat the collectors adsorbed on minerals through van der Waals force and electrostatic interaction. The physical method includes vacuum, ultrasonic, heating, centrifugation, regrinding, stirring, concentration, activated carbon, and nanobubbles and so on [20–24]. However, when the groups of collectors have strong chemical interaction with the active sites on minerals, the desorption efficiencies of collectors using the physical methods are poor. Therefore, in order to improve the desorption efficiencies of collectors, chemical reagents have to be added for destroying the adsorption structures of collectors on minerals. The chemical reagents include strong acids, strong bases, sodium sulfide, hydrogen peroxide, and other strong oxidants [25–27]. Due to the addition of chemical reagents, the cost of the chemical method is generally higher than that of the physical method, and it is easy to cause secondary pollution. Hence, in order to improve the desorption efficiencies of collectors and save costs, the physical method and chemical method are usually used together in the industry.

However, the existing desorption methods of collectors rely too much on instruments and chemical reagents, resulting in the desorption efficiencies of collectors remaining low. Moreover, the desorbed collectors cannot be reused. Therefore, in this study, the effect of the Pb-BHA-NaOL collector on scheelite and fluorite floatability was first studied to obtain the scheelite concentrate at the optimal flotation conditions. On this basis, the desorption tests of Pb and BHA from the surfaces of scheelite concentrate were implemented. The content of NaOL in the Pb-BHA-NaOL collector with a 240:120:1 molar ratio was very small, so the desorption amount of NaOL in the desorption tests was not detected. After solid-liquid separation, the desorption solution composed of Pb and BHA was reused for scheelite and fluorite flotation. The desorption performance of this collector was analyzed through Fourier transform infrared spectroscopy (FTIR) measurements and atomic force microscopy (AFM) imaging.

2. Materials and Methods

2.1. Materials and Reagents

Scheelite and fluorite crystals from Chenzhou, China were crushed, ground, and then screened using a Tyler sieve. The $-74 + 38$ μm fraction was utilized to implement the tests of flotation, desorption, and reuse. The -5 μm fraction obtained by further grinding was used in FTIR measurements. The X-ray diffraction (XRD) results in Figure 1 suggest that the purity of both minerals was very high; the scheelite and fluorite purity acquired through the chemical analysis was 98% and 99%, respectively. The real ore with a concentration of 50%, a fineness of 80% passing -74 μm, and a grade of WO_3 0.34% was derived from the Dongbo dressing plant in Chenzhou. Other properties of the real ore are shown in Tables 1 and 2. Pb ($Pb(NO_3)_2$), BHA ($C_7H_7NO_2$), and NaOL ($C_{17}H_{33}CO_2Na$) were analytically pure and taken from TCI Co., Ltd., Tokyo, Japan. The slurry pH was adjusted by HCl and NaOH solutions.

Table 1. Results of chemical multi-element analysis of the real ore.

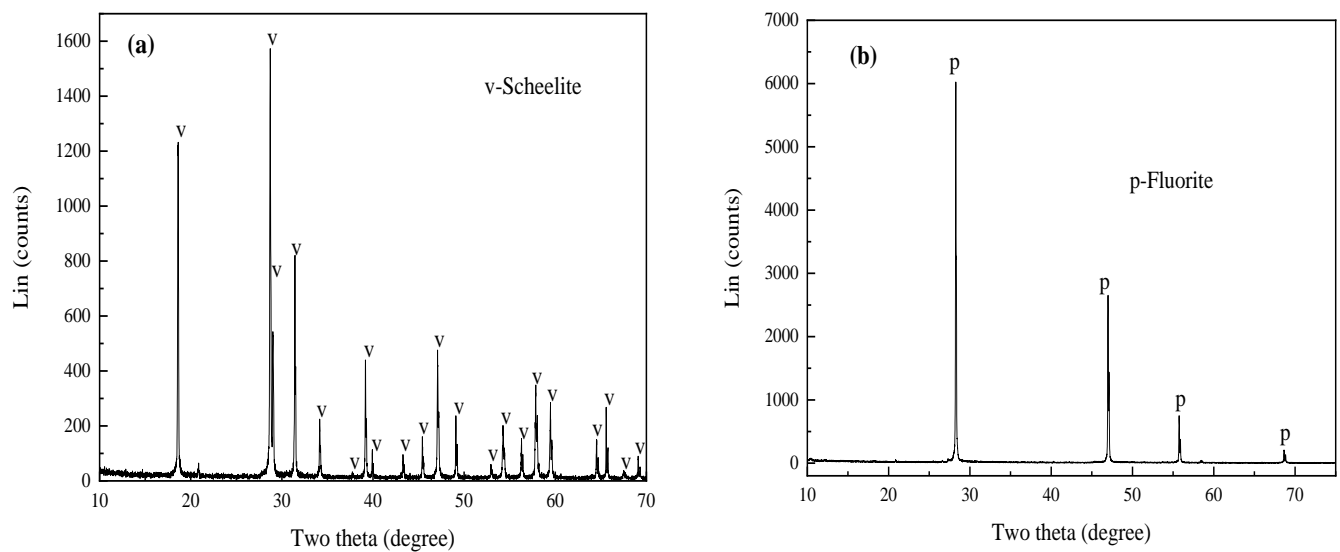| Element	Content (%)	Element	Content (%)
MgO	0.94	WO_3	0.34
CaO	30.35	Mo	0.09
Al_2O_3	5.50	Bi	0.10
SiO_2	27.60	S	0.79
CaF_2	21.66	Fe	8.22
Sn	0.11	Cu	0.022

Figure 1. XRD spectra of scheelite (**a**) and fluorite (**b**).

Table 2. Major minerals and their relative contents in the real ore.

Mineral	Content (%)	Mineral	Content (%)
Scheelite	0.37	Sericite	4.50
Wolframite	0.05	Chlorite	3.50
Cassiterite	0.09	Hornblende	2.00
Molybdenite	0.14	Kaolinite	2.00
Bismuthinite	0.08	Feldspar	2.00
Native bismuth	0.02	Diopside	1.50
Magnetite	2.00	Idocrase	0.50
Pyrite	1.25	Calcite	7.00
Fluorite	21.50	Dolomite	1.00
Quartz	20.00	Others	0.50
Garnet	30.00	Total	100.00

2.2. Desorption and Reuse Tests

Pure mineral flotation tests were executed via an XFG flotation machine with a 40 mL plexiglass cell filled with 2.00 g of the mineral sample and 35 mL of deionized (DI) water. The detailed flotation, collector desorption, and reuse flowsheets of pure minerals are shown in Figure 2. Note that the XFG flotation machine was also used in the agitation in the desorption tests. The related flotation, collector desorption, and reuse flowsheets of the real ore using an XFD flotation machine are presented in Figure 3. Note that the desorption efficiency (*E*) of Pb or BHA was calculated by Equation (1). The contents of Pb and BHA were respectively determined by inductively coupled plasma optical emission spectrometer (ICP-OES, Thermo Fisher Scientific, Waltham, MA, USA) and ultraviolet-visible photometer (UV-2600, Shimadzu, Japan).

$$E = \frac{A_d}{A_t} \times 100\%, \tag{1}$$

where A_d represents the desorption amount of Pb or BHA; A_t denotes the total adsorption amount of Pb or BHA on the scheelite concentrate surfaces.

2.3. FTIR Measurements

FTIR measurements were performed via a Nexus 670 infrared spectrometer (Thermo Nicolet Corporation, Madison, WI, USA). The scheelite concentrate with a particle size of −5 µm was obtained according to the flowsheet except for the terpineol and flotation links in Figure 2. The scheelite sample after the desorption of the collector was acquired when

the scheelite concentrate was treated through a strong stirring for 15 min at pH 13.0 and a speed of 1600 r/min. Then, these samples were dried, ground with the spectral grade KBr powder, and measured.
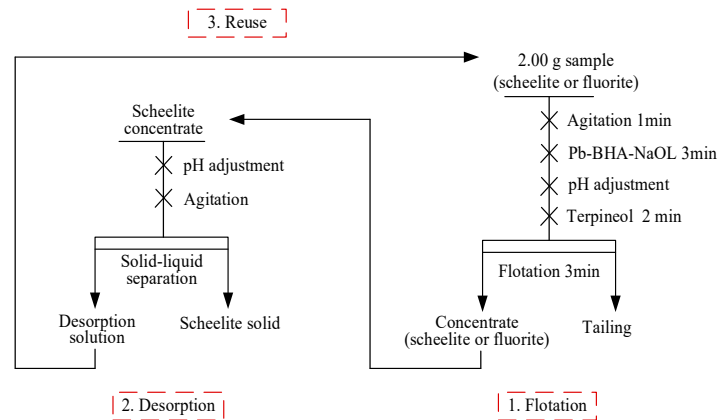

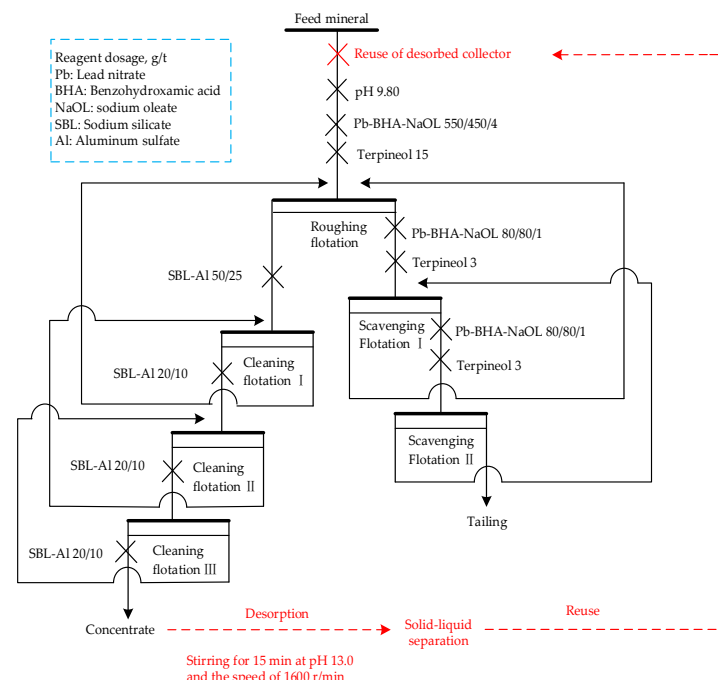**Figure 2.** Flowsheets of desorption and reuse tests of pure mineral.

Figure 3. Flowsheets of desorption and reuse tests of the real ore.

2.4. AFM Imaging

AFM imaging analysis was implemented using the Multimode SPM AFM (Veeco Instruments Inc., Plainview, NY, USA) with a tapping mode at 25 °C. The test probe (RTESP-300) was a single-crystal silicon probe with a resonance frequency of 286 KHz. The scheelite (112) surface of the scheelite crystal was confirmed by XRD; the surface was then polished and cleaned with a semi-automatic polishing machine (Tegramin-25, Struers). The freshly cleaved scheelite sample was treated using the same method as the sample of FTIR measurements to acquire scheelite concentrates before and after the desorption of collector. These samples were then dried through a high-purity nitrogen before testing.

3. Results and Discussion

3.1. Desorption and Reuse Experiment Results

Figure 4 demonstrates the scheelite and fluorite recoveries as a function of the slurry pH when using the Pb-BHA-NaOL collector. At pH 9.0, there was the maximum difference in the recovery between scheelite and fluorite using 2.4×10^{-4} mol/L (M) Pb, 1.2×10^{-4} M BHA, and 1.0×10^{-6} M NaOL. Moreover, the scheelite recovery declined rapidly when the slurry pH value was over 9.0, suggesting that the Pb-BHA-NaOL collector might have low adsorption on the scheelite surfaces. This result also provides a direction for the desorption of this collector from the scheelite concentrate surfaces.
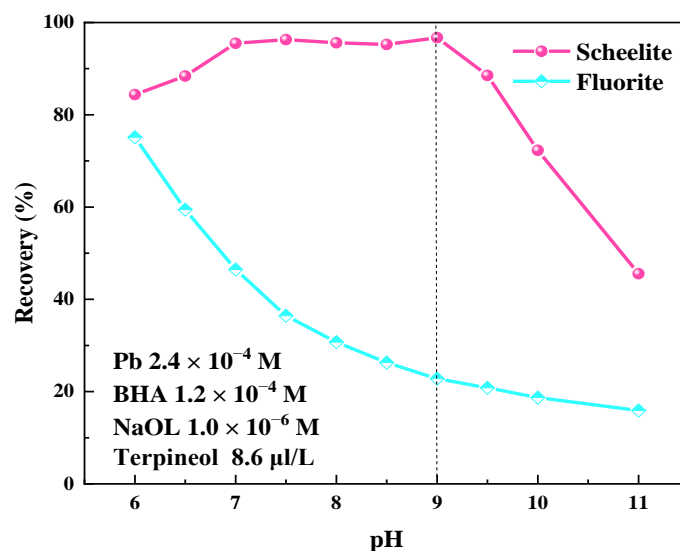

Figure 4. Scheelite and fluorite recoveries as a function of the slurry pH using the Pb-BHA-NaOL collector.

Considering that the costs and contents of Pb and BHA in the Pb-BHA-NaOL collector are far higher than those of NaOL, this manuscript mainly studied the desorption and reuse of Pb and BHA from the scheelite concentrate surfaces. Figures 5 and 6 show the effect of the slurry pH and stirring conditions on the desorption efficiencies of Pb and BHA, respectively.
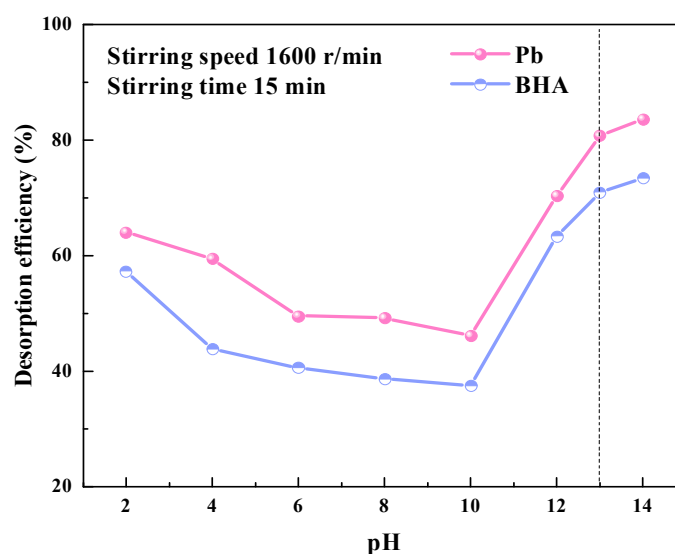

Figure 5. Effect of the slurry pH on the desorption efficiencies of Pb and BHA from the scheelite concentrate surfaces.
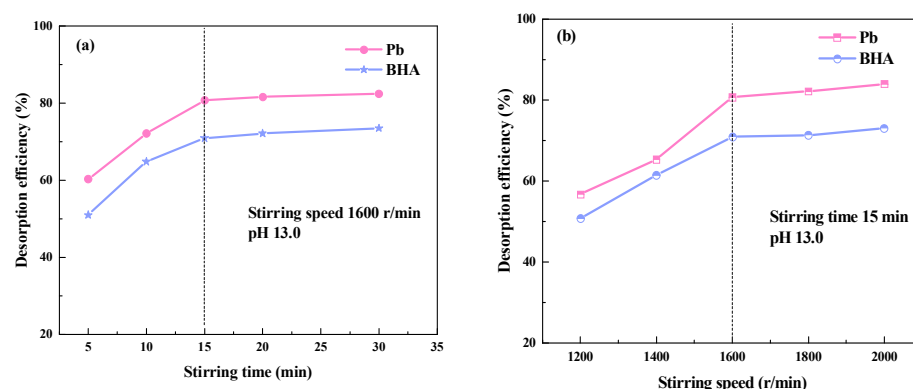
Figure 6. Effect of the stirring conditions on the desorption efficiencies of Pb and BHA from the scheelite concentrate surfaces. (**a**) Stirring time; (**b**) Stirring speed.

In Figure 5, the desorption efficiencies of Pb and BHA first declined and then rose with the increase in pH values. The desorption efficiencies of Pb and BHA were not significantly improved after the pH value was greater than 13.0. Thus, in consideration of the costs and desorption efficiencies of Pb and BHA, the preferred pH value was 13.0.

Figure 6a,b present the effect of the stirring time and speed on the desorption efficiencies of Pb and BHA at pH 13.0, respectively. The desorption efficiencies of Pb and BHA gradually raised before the stirring time and speed were not greater than 15 min and 1600 r/min, respectively. Therefore, the best desorption efficiencies of Pb and BHA were 80.71% and 70.93% at the pH value of 13.0 and stirring conditions of 15 min and 1600 r/min, respectively. As shown in Figure 2, after solid-liquid separation, the corresponding contents of Pb and BHA in the original desorption solution were 1.6×10^{-4} and 5.0×10^{-5} M, respectively.

Figure 4 demonstrates that obtaining the maximum difference in the recovery between scheelite and fluorite required 2.4×10^{-4} M Pb and 1.2×10^{-4} M BHA, respectively. Considering the contents of Pb and BHA in the original desorption solution (1.6×10^{-4} and 5.0×10^{-5} M), around 8.0×10^{-5} M Pb and 7×10^{-5} M BHA might be supplemented to obtain the similar floatability difference of both minerals when the desorbed Pb and BHA were reused. Consequently, scheelite and fluorite recoveries as a function of the supplementary dosages of Pb and BHA were investigated, as demonstrated in Figure 7.
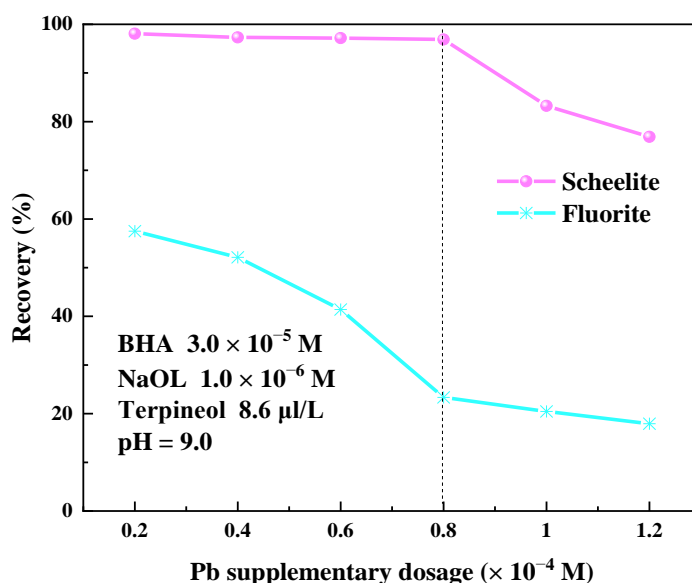

Figure 7. Effect of the supplementary dosage of Pb on scheelite and fluorite recoveries in the presence of the reuse of desorbed Pb and BHA.

Figure 7 displays that, when reusing the desorbed Pb and BHA original solution activated with nitric acid, the scheelite recovery remained around 97% until the supplementary dosages of Pb and BHA did not exceed 8.0×10^{-5} M and 3.0×10^{-5} M, respectively. The fluorite recovery gradually decreased in the whole range of the supplementary dosages of the two reagents. Therefore, the optimal supplementary dosages of Pb and BHA were 8.0×10^{-5} and 3.0×10^{-5} M, respectively. When the concentrations of desorbed Pb and BHA were taken into account, the corresponding total concentrations of Pb and BHA were 2.4×10^{-4} and 8.0×10^{-5} M, respectively. In other words, the dosages Pb and BHA could be respectively saved by 67% and 75% in the presence of the reuse of desorbed Pb and BHA. Additionally, the total concentrations of Pb and BHA (2.4×10^{-4} and 8.0×10^{-5} M) were also close to the initial concentrations of Pb and BHA (2.4×10^{-4} and 1.2×10^{-4} M), suggesting a perfect result of the desorption and reuse of Pb and BHA.

According to Figure 3, after the collector on the actual scheelite concentrate surfaces was desorbed and reused, the dosages of Pb and BHA used for roughing flotation could be respectively reduced from the initial 550 and 450 g/t to 400 and 290 g/t. Note that the recovery and grade of the scheelite concentrate before and after the reuse of the collector should be similar and the dosage of NaOL should remain unchanged. This result proves that the collector desorption and reuse in the real ore could economize on 150 g/t Pb and 160 g/t BHA. Namely, it could save 27.27% Pb and 35.56% BHA, suggesting high feasibility for this technology in industrial applications.

3.2. FTIR Analysis

In Figure 8, the peak at 808.2 cm^{-1} on the bare scheelite surfaces belonged to WO_4^{2-} of scheelite itself [28,29]. After adding the collector, the peaks at 1597.1, 1384.9, and 1153.4 cm^{-1} on the scheelite concentrate surfaces belonged to the stretching vibrations of C=O, Pb-O, and C-N groups in this collector [30,31]. However, after the treatment of strong alkali (pH 13.0) and 15 min of stirring at a speed of 1600 r/min, the peaks of these groups (C=O, Pb-O, and C-N) on the scheelite concentrate surfaces obviously weakened or disappeared. This result implies that Pb and BHA had significant desorption from the scheelite concentrate surfaces, agreeing well with the flotation results in Figures 5 and 6.
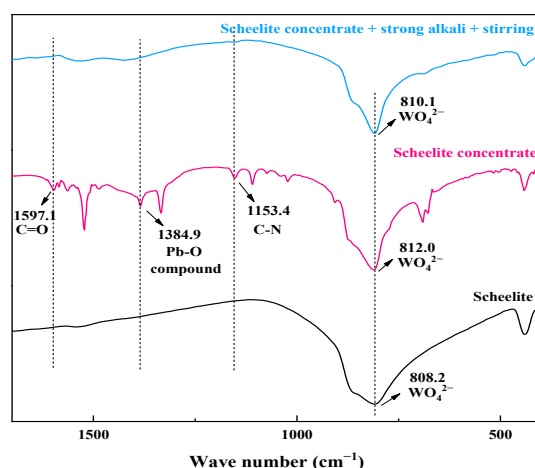

Figure 8. FTIR spectra of the bare scheelite and scheelite concentrate before and after the desorption of Pb and BHA.

3.3. AFM Analysis

FTIR analysis exhibited the changes in the scheelite concentrate surfaces before and after the desorption of Pb and BHA from the perspective of spectroscopy. In order to further observe the surface changes from a more microscopic perspective, AFM imaging was carried out. The (112) plane is the most commonly exposed surface of scheelite [32]. Consequently, the AFM 2D images, 3D images and adsorption height curves of the Pb-BHA-NaOL collector on this plane are presented in Figure 9.
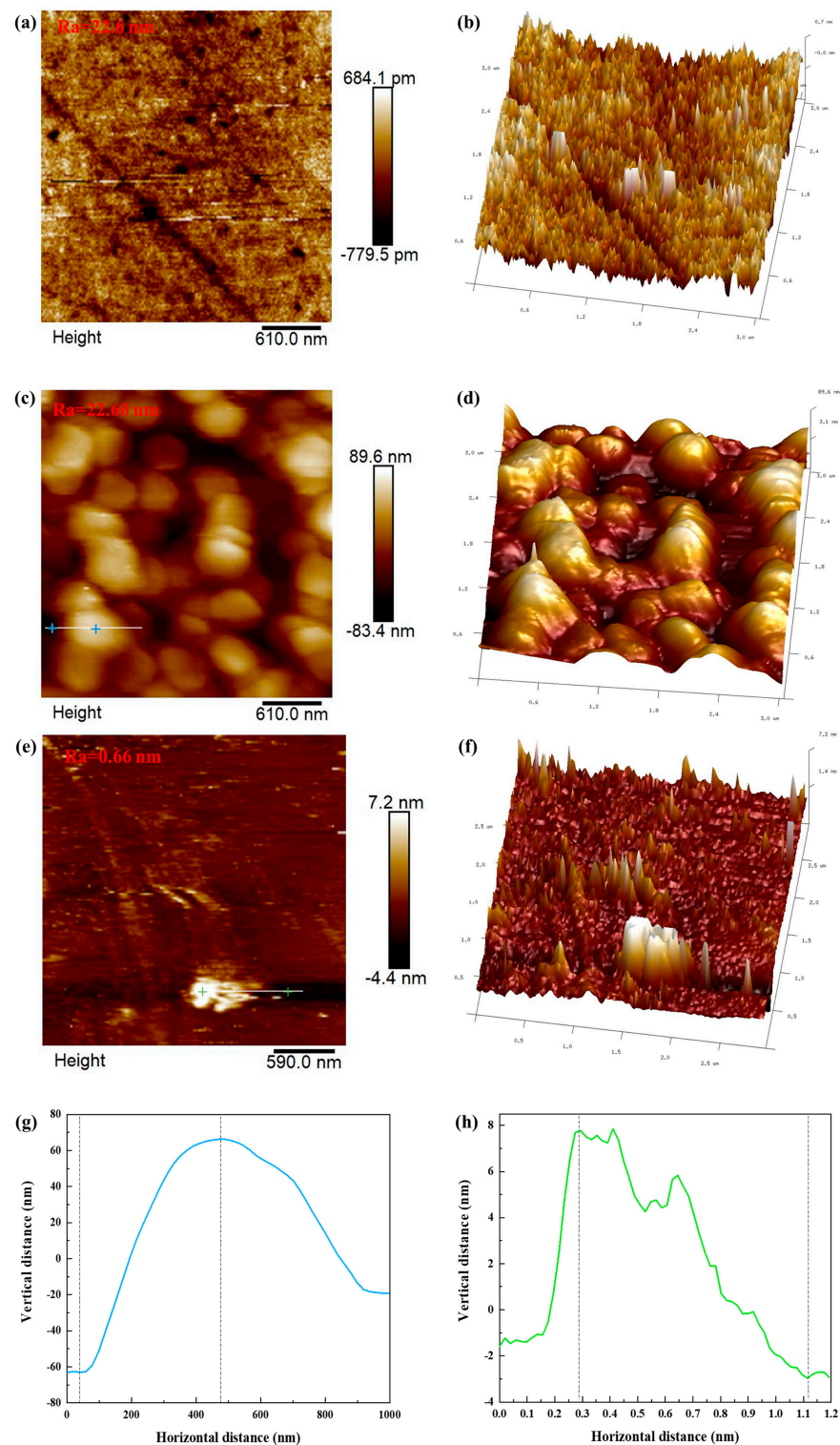
Figure 9. AFM 2D images, 3D images and adsorption height curves of Pb-BHA-NaOL collector on the scheelite (112) surface. (**a**,**b**) 2D and 3D images of the bare scheelite (112) surface; (**c**,**d**) 2D and 3D images of the scheelite (112) surface before desorption of Pb and BHA; (**e**,**f**) 2D and 3D images of the scheelite (112) surface after desorption of Pb and BHA; (**g**,**h**) Adsorption height curves of Pb-BHA-NaOL collector on the scheelite (112) surface before and after desorption of Pb and BHA.

Compared with the roughness (R_a), 2D and 3D images of the bare scheelite (112) surface in Figure 9a,b, the scheelite (112) surface before the desorption of Pb and BHA in Figure 9c,d had a greater R_a and obvious bulges (22.60 nm), suggesting a large amount

of Pb and BHA adsorption on the scheelite (112) surface. After the desorption of Pb and BHA, the R_a of the scheelite (112) surface in Figure 9e was greatly reduced to 0.66 nm, which was close to that of the bare scheelite (112) surface. Moreover, the absolute value of the height difference of the collector adsorption on the scheelite (112) surface before the desorption of Pb and BHA in Figure 9g was 129.28 nm, much more than that after the desorption of Pb and BHA in Figure 9h (12.87 nm). These results reveal that Pb and BHA were efficiently desorbed from the scheelite (112) surface using the method in Figure 2, in line with the FTIR analysis in Figure 8. Furthermore, the model of the desorption and reuse of the Pb-BHA-NaOL collector is exhibited in Figure 10.
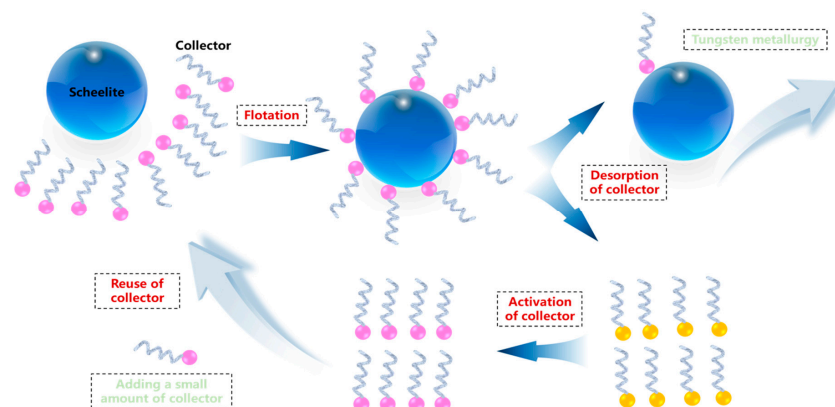

Figure 10. Model of the desorption and reuse of Pb-BHA-NaOL collector on scheelite.

4. Conclusions

The Pb-BHA-NaOL collector with a 240:120:1 molar ratio had high selectivity and strong collecting ability in scheelite flotation, but Pb and BHA in this collector also have the common defects of flotation reagents including high cost, environmental pollution and reducing concentrate hydrometallurgy efficiency. Therefore, taking scheelite and this collector as an example, the idea of efficient desorption and reuse of a collector from the mineral concentrate surfaces was first proposed and implemented. The Pb and BHA in this collector could be efficiently desorbed from the scheelite concentrate surfaces through strong stirring for 15 min at pH 13.0 and a speed of 1600 r/min. The reuse of desorbed Pb and BHA could save 67% Pb and 75% BHA in scheelite flotation, respectively. Moreover, the desorption and reuse method of this collector was also verified using the real ore, which could economize on 150 g/t Pb and 160 g/t BHA. FTIR analysis revealed that Pb-O, C=O, and C-N groups of Pb and BHA adsorbed on the scheelite surfaces obviously weakened or disappeared. AFM analysis further confirmed that most of the Pb and BHA on the scheelite surfaces were removed.

Therefore, in this work, the efficient desorption and reuse of Pb and BHA can not only reduce the cost of flotation reagents but also help to improve the environment and tungsten hydrometallurgy efficiency. In addition, the idea proposed in this manuscript also provides a reference for the desorption and reuse of other flotation reagents.

Author Contributions: Conceptualization, J.W., Z.G. and W.S.; methodology, J.W.; investigation, J.W.; writing—original draft preparation, J.W.; writing—review and editing, Z.G. and W.S. All authors have read and agreed to the published version of the manuscript.

Data Availability Statement: Not applicable.

Conflicts of Interest: The authors declare no conflict of interest.

References

1. Miao, Z.; Tao, L.; Wang, J.; Jiang, Z.; Peng, T.; Sun, W.; Gao, Z. Selective separation of fluorite from scheelite using N-decanoylsarcosine sodium as a novel collector. *Minerals* **2022**, *12*, 855. [CrossRef]
2. Zhao, C.; Sun, C.; Zhu, Y.; Zhu, Y.; Yin, W. Study of the mechanism of the fe-bha chelates in scheelite flotation. *Minerals* **2022**, *12*, 484. [CrossRef]
3. Foucaud, Y.; Filippov, L.; Filippova, I.; Badawi, M. The challenge of tungsten skarn processing by froth flotation: A review. *Front. Chem.* **2020**, *8*, 230. [CrossRef]
4. Kupka, N.; Rudolph, M. Froth flotation of scheelite–A review. *Int. J. Min. Sci. Technol.* **2018**, *28*, 373–384. [CrossRef]
5. Zhang, H.; Sun, W.; Zhu, Y.; He, J.; Chen, D.; Zhang, C. Effects of the goethite surface hydration microstructure on the adsorption of the collectors dodecylamine and sodium oleate. *Langmuir* **2021**, *37*, 10052–10060. [CrossRef]
6. Wei, Z.; Hu, Y.; Han, H.; Sun, W.; Wang, R.; Sun, W.; Wang, J.; Gao, Z.; Wang, L.; Zhang, C. Selective separation of scheelite from calcite by self-assembly of H_2SiO_3 polymer using Al^{3+} in Pb-BHA flotation. *Minerals* **2019**, *9*, 43. [CrossRef]
7. Wei, Z.; Fu, J.; Han, H.; Sun, W.; Yue, T.; Wang, L.; Sun, L. A highly selective reagent scheme for scheelite flotation: Polyaspartic acid and Pb–BHA complexes. *Minerals* **2020**, *10*, 561. [CrossRef]
8. Jung, M.Y.; Park, J.H.; Yoo, K. Effects of ferrous sulfate addition on the selective flotation of scheelite over calcite and fluorite. *Minerals* **2020**, *10*, 864. [CrossRef]
9. Zhao, C.; Sun, C.; Yin, W.; Luo, B. An investigation of the mechanism of using iron chelate as a collector during scheelite flotation. *Miner. Eng.* **2019**, *131*, 146–153. [CrossRef]
10. Wu, Q.; Zhu, Y.; Sun, W.; Xie, R.; Li, Y.; Han, Y. Adsorption mechanism of efficient flotation separation of scheelite from calcite by a novel mixed collector. *J. Mol. Liq.* **2022**, *345*, 116994. [CrossRef]
11. Xu, Y.; Xu, L.; Wu, H.; Wang, Z.; Shu, K.; Fang, S.; Zhang, Z. Flotation and co–adsorption of mixed collectors octanohydroxamic acid/sodium oleate on bastnaesite. *J. Alloys Compd.* **2020**, *819*, 152948. [CrossRef]
12. Xu, L.; Tian, J.; Wu, H.; Lu, Z.; Yang, Y.; Sun, W.; Hu, Y. Effect of Pb^{2+} ions on ilmenite flotation and adsorption of benzohydroxamic acid as a collector. *Appl. Surf. Sci.* **2017**, *425*, 796–802. [CrossRef]
13. Wang, J.; Gao, Z.; Gao, Y.; Hu, Y.; Sun, W. Flotation separation of scheelite from calcite using mixed cationic/anionic collectors. *Miner. Eng.* **2016**, *98*, 261–263. [CrossRef]
14. Wang, J.; Gao, Z.; Han, H.; Sun, W.; Gao, Y.; Ren, S. Impact of NaOL as an accelerator on the selective separation of scheelite from fluorite using a novel self-assembled Pb-BHA-NaOL collector system. *Appl. Surf. Sci.* **2021**, *537*, 147778. [CrossRef]
15. Jin, S.; Ou, L. Comparison of the effects of sodium oleate and benzohydroxamic acid on fine scheelite and cassiterite hydrophobic flocculation. *Minerals* **2022**, *12*, 687. [CrossRef]
16. Meng, X.; Khoso, S.A.; Jiang, F.; Zhang, Y.; Yue, T.; Gao, J.; Lin, S.; Liu, R.; Gao, Z.; Chen, P. Removal of chemical oxygen demand and ammonia nitrogen from lead smelting wastewater with high salts content using electrochemical oxidation combined with coagulation–flocculation treatment. *Sep. Purif. Technol.* **2020**, *235*, 116233. [CrossRef]
17. Wang, H.; Wang, S.; Wang, S.; Fu, L.; Zhang, L. Efficient metal-organic framework adsorbents for removal of harmful heavy metal Pb (II) from solution: Activation energy and interaction mechanism. *J. Environ. Chem. Eng.* **2023**, *11*, 109335. [CrossRef]
18. Li, B.; Zhang, X.; Tefsen, B.; Wells, M. From speciation to toxicity: Using a "Two-in-One" whole-cell bioreporter approach to assess harmful effects of Cd and Pb. *Water Res.* **2022**, *217*, 118384. [CrossRef]
19. Zhu, S.; Xia, M.; Chu, Y.; Khan, M.A.; Lei, W.; Wang, F.; Muhmood, T.; Wang, A. Adsorption and desorption of Pb (II) on l-lysine modified montmorillonite and the simulation of interlayer structure. *Appl. Clay Sci.* **2019**, *169*, 40–47. [CrossRef]
20. Zhou, W.; Liu, K.; Wang, L.; Zhou, B.; Niu, J.; Ou, L. The role of bulk micro-nanobubbles in reagent desorption and potential implication in flotation separation of highly hydrophobized minerals. *Ultrason. Sonochem.* **2020**, *64*, 104996. [CrossRef]
21. Jiang, Y.; Chen, Y.; Zi, F.; Hu, X.; Chen, S.; He, P.; Zhao, L.; Li, X.; Li, J.; Lin, Y. Making untreated carbon effective in cleaner thiosulfate system: A new and high-efficiency method including gold adsorption and desorption. *J. Clean. Prod.* **2022**, *334*, 130185. [CrossRef]
22. Elwakeel, K.Z.; Shahat, A.; Al-Bogami, A.S.; Wijesiri, B.; Goonetilleke, A. The synergistic effect of ultrasound power and magnetite incorporation on the sorption/desorption behavior of Cr (VI) and As (V) oxoanions in an aqueous system. *J. Colloid Interf. Sci.* **2020**, *569*, 76–88. [CrossRef] [PubMed]
23. Li, J.; Zhou, W.; Su, Y.; Zhao, Y.; Zhang, W.; Xie, L.; Meng, X.; Gao, J.; Sun, F.; Wang, P. The enhancement mechanism of the microwave-assisted toluene desorption for activated carbon regeneration based on the constructive interference. *J. Clean. Prod.* **2022**, *378*, 134542. [CrossRef]
24. Liu, P.; Liu, C.; Hu, T.; Shi, J.; Zhang, L.; Liu, B.; Peng, J. Kinetic study of microwave enhanced mercury desorption for the regeneration of spent activated carbon supported mercuric chloride catalysts. *Chem. Eng. J.* **2021**, *408*, 127355. [CrossRef]
25. Kang, J.; Chen, C.; Sun, W.; Tang, H.; Yin, Z.; Liu, R.; Hu, Y.; Nguyen, A.V. A significant improvement of scheelite recovery using recycled flotation wastewater treated by hydrometallurgical waste acid. *J. Clean. Prod.* **2017**, *151*, 419–426. [CrossRef]

26. Khoso, S.A.; Hu, Y.; Fei, L.; Ya, G.; Liu, R.; Wei, S. Xanthate interaction and flotation separation of H_2O_2-treated chalcopyrite and pyrite. *T. Nonferr. Metal. Soc.* **2019**, *29*, 2604–2614. [CrossRef]

27. Nchoe, O.B.; Ntuli, T.D.; Klink, M.J.; Mtunzi, F.M.; Pakade, V.E. A comparative study of acid-treated, base-treated, and Fenton-like reagent-treated biomass for Cr (VI) sequestration from aqueous solutions. *Water Environ. Res.* **2021**, *93*, 370–383. [CrossRef]

28. Zhang, C.; Wu, H.; Sun, W.; Hu, Y.; Wang, C.; Zhu, S.; Chen, P. Investigation of the flotation separation of scheelite from fluorite with a novel chelating agent: Pentasodium diethylenetriaminepentaacetate. *Minerals* **2022**, *12*, 530. [CrossRef]

29. Bo, F.; Xianping, L.; Jinqing, W.; Pengcheng, W. The flotation separation of scheelite from calcite using acidified sodium silicate as depressant. *Miner. Eng.* **2015**, *80*, 45–49. [CrossRef]

30. Han, H.; Xiao, Y.; Hu, Y.; Sun, W.; Nguyen, A.V.; Tang, H.; Gui, X.; Xing, Y.; Wei, Z.; Wang, J. Replacing Petrov's process with atmospheric flotation using Pb-BHA complexes for separating scheelite from fluorite. *Miner. Eng.* **2020**, *145*, 106053. [CrossRef]

31. Goebbert, D.J.; Garand, E.; Wende, T.; Bergmann, R.; Meijer, G.; Asmis, K.R.; Neumark, D.M. Infrared spectroscopy of the microhydrated nitrate ions $NO_3^-(H_2O)_{1-6}$. *J. Phys. Chem. A* **2009**, *113*, 7584–7592. [CrossRef] [PubMed]

32. Wang, J.; Li, W.; Zhou, Z.; Gao, Z.; Hu, Y.; Sun, W. 1-Hydroxyethylidene-1, 1-diphosphonic acid used as pH–dependent switch to depress and activate fluorite flotation I: Depressing behavior and mechanism. *Chem. Eng. Sci.* **2020**, *214*, 115369. [CrossRef]